JNCI Cancer Spectrum (2021) 5(5): pkab069

doi: 10.1093/jncics/pkab069
First published online 11 August 2021
Systematic Review

Structural and Functional Brain Imaging in Long-Term Survivors of Childhood Acute Lymphoblastic Leukemia Treated With Chemotherapy: A Systematic Review

Kellen Gandy, PhD,[1] Matthew A. Scoggins, PhD,[2] Lisa M. Jacola, PhD,[3] Molly Litten, BS,[1] Wilburn E. Reddick, PhD,[2,*] Kevin R. Krull, PhD[1,3]

[1]Department of Epidemiology and Cancer Control, St. Jude's Children's Research Hospital, Memphis, TN, USA, [2]Department of Diagnostic Imaging, St. Jude's Children's Research Hospital, Memphis, TN, USA, and [3]Department of Psychology, St. Jude's Children's Research Hospital, Memphis, TN, USA

[*]**Correspondence to:** Kevin Krull, PhD, Department of Epidemiology and Cancer Control, St. Jude Children's Research Hospital, 262 Danny Thomas Pl, Mail Stop 735, Memphis, TN 38105, USA (e-mail: kevin.krull@stjude.org)

Abstract

Background: The effect of chemotherapy on brain development in long-term survivors of pediatric acute lymphoblastic leukemia (ALL) was systematically reviewed. **Methods:** A systematic search of Pubmed, Scopus, and PsycINFO databases was conducted to identify articles published between January 2000 and February 2020 that implemented magnetic resonance imaging to assess brain structure and function in pediatric ALL survivors (diagnosed younger than 21 years of age). The review included articles that were published on children diagnosed with ALL between 0 and 21 years of age and treated with chemotherapy-only protocols. Articles meeting the inclusion criteria described survivors on average of 5 years or more from diagnosis and were peer-reviewed articles and original studies. **Results:** The search yielded 1975 articles with 23 articles meeting inclusion criteria. The review revealed that survivors had statistically significant alterations in brain anatomy, most commonly a smaller hippocampus and impaired microstructural white matter integrity in frontal brain regions. Survivors also had impaired brain function including lower brain network efficiency and altered resting state connectivity. Survivors also displayed widespread reductions in brain activation (ie, frontal, temporal, parietal brain regions) during cognitive tasks. **Conclusion:** Although the neurotoxic effects of cancer treatment are reduced in the absence of cranial radiation, survivors treated on chemotherapy-only protocols still display long-term alterations in brain structure and function, which contribute to lifelong neurocognitive late effects.

Prophylactic treatment of the central nervous system (CNS) to reduce the risk of relapse in pediatric acute lymphoblastic leukemia (ALL) has dramatically improved 5-year survival rates (1). Over the years, the deleterious effects of cranial radiation therapy (CRT) (2-4) as a method for prophylaxis resulted in the eventual replacement of CRT by risk-stratified intrathecal and high-dose intravenous methotrexate (MTX) (5). Although survival rates improved and neurotoxicity declined, survivors of pediatric ALL treated with chemotherapy-only continue to demonstrate long-term alterations in brain development and function, which correspond with neurocognitive deficits in domains of attention, executive function, and processing speed (6,7). Neurocognitive deficits are initially subtle in survivors, though they can progress over time and have an adverse impact on long-term functional outcomes and quality of life (8). Neurotoxic drugs used in chemotherapy can penetrate the blood-brain barrier (BBB) and cause cytokine-induced inflammation (9), neural apoptosis (10), and inhibit hippocampal neurogenesis (11). These combined effects can have a lasting impact on brain development and function, particularly among pediatric patients who are within a critical time period for brain development. Given that the majority of patients with ALL are diagnosed and treated during early childhood, disruptions in pediatric brain development can have a long-term impact on survivors. To better understand the neurotoxic effects of chemotherapy on brain structure and function, a systematic review was conducted to assess the current literature reporting on magnetic resonance imaging (MRI) in long-term survivors of childhood ALL treated on chemotherapy-only protocols without the use of CRT. This review summarizes the critical findings

Received: 12 February 2021; **Revised:** 19 May 2021; **Accepted:** 11 August 2021

related to chemotherapy-induced brain changes as assessed across various neuroimaging techniques.

Methods

A systematic review was conducted in accordance with the Preferred Reporting Items for Systematic Review and Meta-Analysis (PRISMA) guidelines (12).

Literature Search Strategy

Pubmed, Scopus, and PsycINFO databases were used to search for articles published between January 1, 2000, and February 14, 2020. A combination of the following terms were used: "acute lymphoblastic leukemia" OR "pediatric leukemia" OR "childhood leukemia" OR "pediatric leukemia survivor" OR "childhood leukemia survivor" OR "childhood cancer survivor" AND "magnetic resonance imaging" OR "brain imaging" OR "brain scan" OR "diffusion-weighted imaging" OR "diffusion tensor imaging" OR "functional imaging" OR "blood-oxygen-level-dependent imaging" OR "voxel-based morphometry" OR "leukoencephalopathy" OR "tractography" OR "connectivity" OR "brain structure" OR "brain volume" OR "surface area" OR "cortical thickness" OR "white matter" OR "grey matter" OR "fractional anisotropy" OR "mean diffusivity" OR "axial diffusivity" OR "radial diffusivity" OR "apparent diffusion coefficient".

Study Selection

Study inclusion criteria for the review were as follows: 1) reported on children diagnosed with ALL between 0 and 21 years of age who were treated with chemotherapy-only protocols and had no history of CRT or stem cell transplant, 2) described survivors on average of 5 years or more from diagnosis or 2.5 years or more from therapy completion, 3) implemented magnetic resonance imaging (MRI) to assess brain structure or function, 4) were peer-reviewed articles written in English, and 5) were original research studies. Case studies, case series (sample size < 20), abstracts, reviews, meta-analyses, commentaries, and qualitative studies were excluded. A secondary search of the articles referenced in original papers meeting the inclusion criteria was also conducted. Methods of the analysis and inclusion criteria were specified in advance.

Data Extraction

The titles and abstracts were extracted for articles yielded from these search terms, and each was reviewed by 3 of the authors (KG, ML, KK) for inclusion or exclusion. Articles meeting initial inclusion were subsequently screened based on the full manuscript to determine the final eligibility. Any disagreements between reviewers were presented and discussed by the group, and a consensus was reached. The risk of bias for each article that met the inclusion criteria was determined using the standardized Risk of Bias in Systematic Reviews (ROBIS) tool (13). Risk of bias was assessed across 4 domains related to: 1) study eligibility criteria, 2) identification and selection of studies, 3) data collection and study appraisal, and 4) synthesis and findings. The risk of bias for each of the domains, as well as for the overall risk of bias, was rated as unclear, low, or high. Only studies with an overall low risk of bias were included in the synthesis of the systematic review.

Magnetic Resonance Imaging

Neuroimaging investigations provide appropriate mechanisms for understanding brain anatomy, function, and disease pathology (see Figure 1). MRI is a noninvasive technique used for examining the pathology and anatomy of the brain and can be useful for assessing the effects of chemotherapy. Structural MRI, most commonly T1-weighted images, can be analyzed to determine the volumetric changes in the brain related to disease and treatment. Additional MRI sequences with varying contrasts, such as T2-weighted images, T2-weighted images with fluid attenuation, and double inversion recovery images that attenuate fluid and normal white matter, can be applied to the analysis to improve intensity-based brain segmentation, particularly for white matter hyperintensities (ie, leukoencephalopathy) (14). Furthermore, the high-resolution T1-weighted scans can be used to register other imaging sequences that probe microstructure and brain connectivity such as diffusion tensor imaging (DTI) and functional MRI (fMRI).

A common approach for analyzing brain structure uses an unbiased whole-brain analysis technique known as voxel-based morphometry (15). This approach involves spatially normalizing high-resolution structural brain scans into a standard stereotactic space template followed by an automated brain segmentation of grey and white matter for cortical and subcortical regions and smoothing using an isotropic Gaussian kernel. Voxel-wise comparisons of grey and white matter are then computed, while controlling for multiple comparisons, to evaluate structural differences between individuals (16). Morphometric properties, such as brain volume and cortical thickness, can be measured using a freely available image analysis suite known as Freesurfer (17). Briefly, the process involves removal of nonbrain tissue using a hybrid watershed and surface deformation procedure (18), automated Talairach transformation, segmentation of the subcortical white matter and deep grey matter volumetric structures (19,20), and automated topology correction (21). Once the cortical models are complete, a variety of deformable procedures can be performed for further data processing and analysis including parcellation of the cerebral cortex into units with respect to gyral and sulcal structure (22,23). Manual segmentation of the brain can also be performed if investigating brain regions that are not included in the atlases (ie, anatomical priors) used for automated segmentation. Manual segmentation techniques are prone to errors in intra- and interrated reliability, which can impact the validity of the results. However, individuals with expertise in brain anatomy and segmentation tools can overcome these barriers by having multiple raters involved in the analysis and repeating the procedures to establish internal consistency (24). These volumetric-based approaches are sufficient to detect subtle changes in brain architecture, making it a suitable technique for investigating the effects of chemotherapy on neuroanatomy in survivors of childhood cancer.

Diffusion-weighted MRI techniques, such as DTI, can also be used to investigate the microstructural properties of white matter within the brain (25). White matter in the brain is composed of myelinated axons that support neural communication between different brain regions. The myelin sheath facilitates neural transmission and protects the axon bundles (ie, white matter tracts) from neurotoxic agents. White matter integrity is

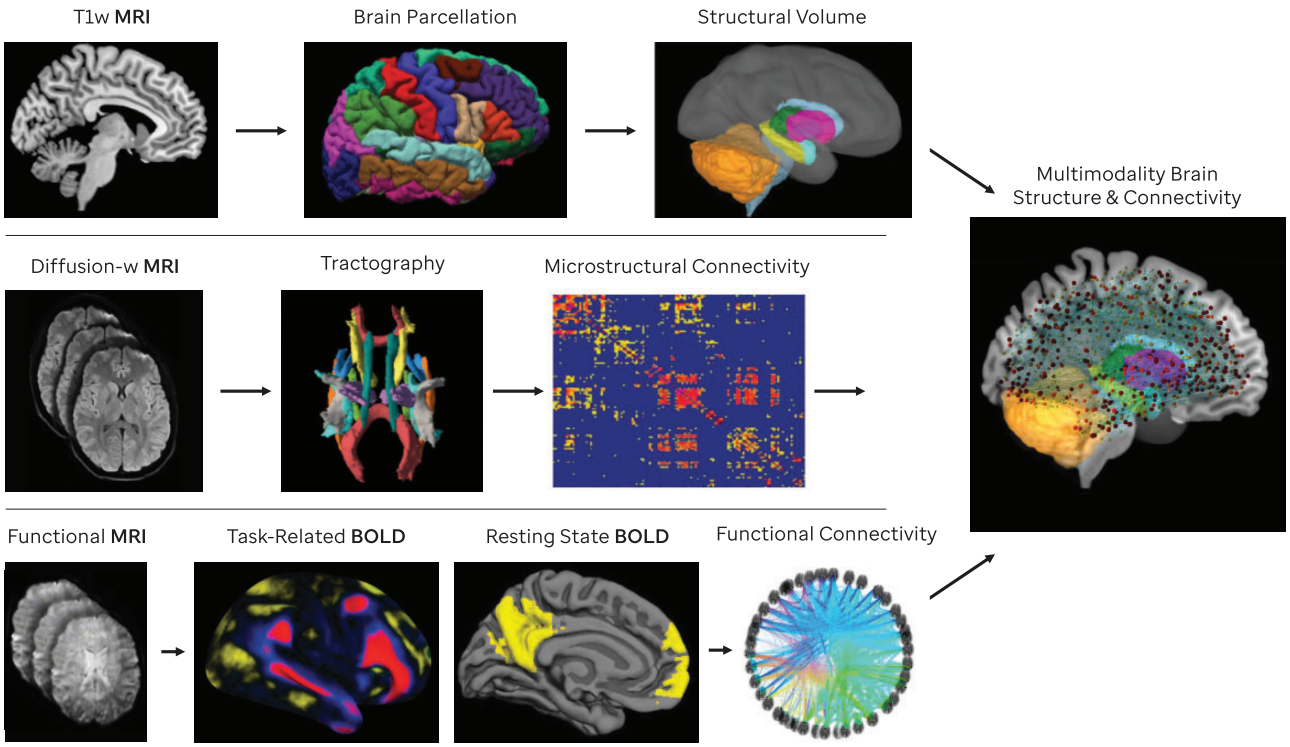

Figure 1. Illustration of different brain MRI modalities and data analysis techniques. BOLD = blood-oxygen-level-dependent; MRI = magnetic resonance imaging.

characterized by the degree of anisotropy and the directional orientation of water diffusion along the tracts (26). Noncompromised white matter tracts typically exhibit increased fractional anisotropy (FA) and decreased directional diffusivity (radial diffusivity, axial diffusivity, mean diffusivity) in comparison to grey matter, which varies with age. Fractional anisotropy is highly sensitive to microstructural changes but less sensitive to the type of change, so directional diffusivity (radial, axial, mean) is often reported in conjunction with FA. Diffusion-weighted images can also be used to perform deterministic or probabilistic tractography to assess alterations in white matter microstructure (27). White matter tracts are analyzed based on anatomical priors and represent the connections between cortical or subcortical regions. Diffusion-weighted connectivity patterns and connectome-based analyses are often assessed using measures derived from graph metric analyses. Given that chemotherapy has a detrimental impact on the CNS, including white matter in the brain, diffusion-weighted approaches provide a suitable mechanism for detecting white matter injury in pediatric cancer survivors treated with CNS-directed chemotherapy.

Functional characteristics of the brain can be measured using fMRI, a technique that measures hemodynamic changes in blood-oxygen-level-dependent (BOLD) signaling, which is related to underlying neural activity. Patterns of brain activation can be evaluated from overt cognitive function (ie, task-based fMRI) or periods of resting quietly (ie, resting state). Task-based fMRI is commonly used to assess brain regions involved in domain-specific cognitive processes, whereas resting state fMRI is frequently used to assess the functional connectivity or global organization of neural networks irrespective of any specific cognitive demand. Alterations in brain activation and connectivity have been observed in long-term survivors of pediatric leukemia, demonstrating that this approach is useful for detecting functional brain changes associated with chemotherapy.

Results

Study Search and Characteristics

The search yielded 1975 articles with 23 articles meeting inclusion criteria (Figure 2). The majority of studies examined structural MRI (12 of 23; 52.2%) and microstructural white matter integrity using DTI (11 of 23; 47.8%), and fewer studies examined functional brain imaging using fMRI (5 of 23; 21.7%). A subset of studies reported on multiple brain imaging techniques during their investigation (6 of 23; 26.1%). All studies had an overall low risk of bias. The details of articles included in the review are described below based on the imaging modality (ie, structural and functional MRI) and summarized in Table 1 and Figure 3.

Structural MRI

Structural characteristics of the brain (ie, grey and white matter volume, cortical thickness) were assessed using MRI and summarized in Table 1 and Figure 3. Volumetric analyses were used to examine long-term structural brain alterations in survivors of pediatric ALL (29,30,34,37,41-44,46–48). Widespread reductions in grey matter volumes were observed across various brain regions in ALL survivors, but most notably, there were consistent reports of smaller hippocampal volumes compared with age-matched controls (37,42,46,47). Overall cerebral white matter volumes were also smaller in ALL survivors, and survivors displayed a lower ratio of intracranial white matter volume in the frontal and temporal lobes (34,43,44). Regional reductions in white matter volumes were also present (41,46). However, there were some inconsistent reports from studies that did not observe volumetric differences in the thalamus, caudate, putamen, amygdala, total grey matter, and total white matter (30,47,48). Survivors also had thinner cortices in various brain

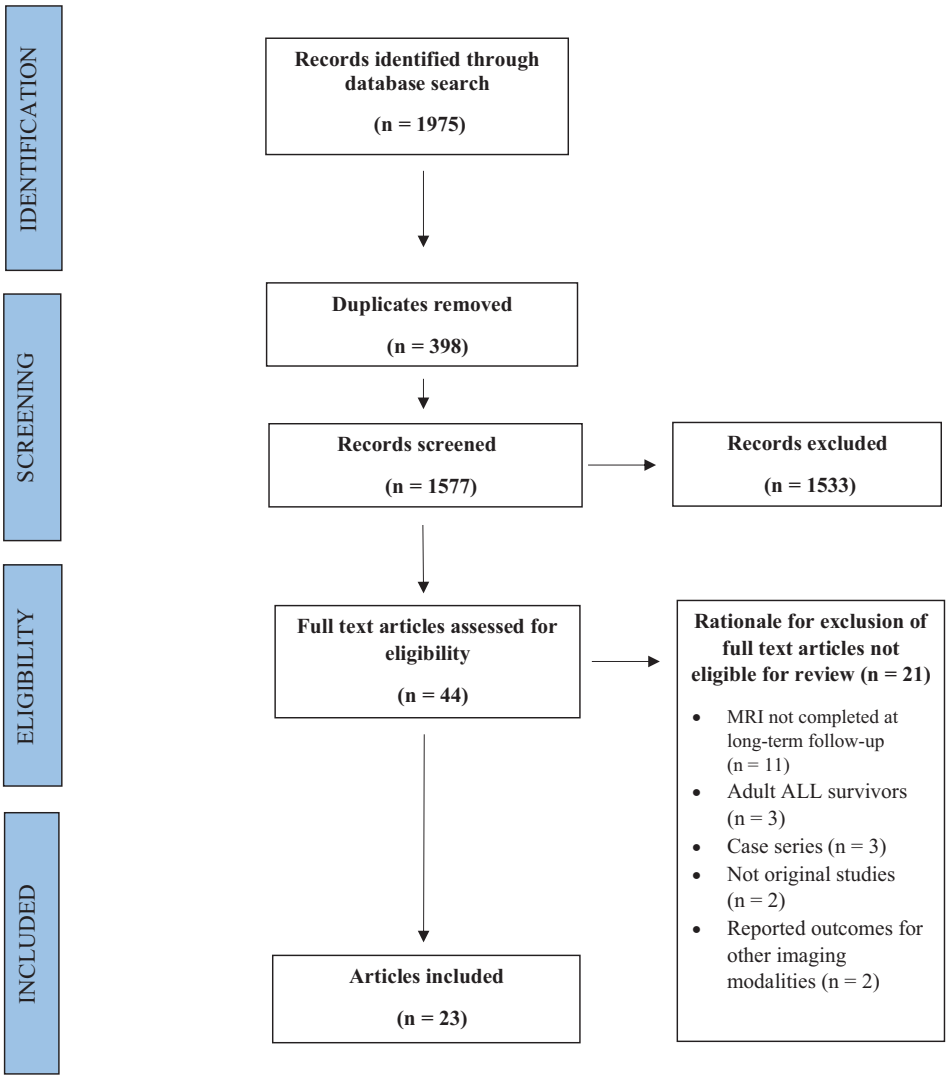

Figure 2. Consort diagram of article screening procedures. ALL = acute lymphoblastic leukemia; MRI = magnetic resonance imaging.

regions (42). Higher dexamethasone exposure was associated with greater cortical thinning in the frontal, temporal, and parietal lobes, particularly among female survivors (42). Additionally, higher plasma concentration of MTX was associated with thicker cortices in the dorsal lateral prefrontal cortex, a region involved in executive functioning (6). Brain abnormalities that were less prevalent, but still observed in ALL survivors, included cerebral microangiopathy, brain atrophy, infarcts, and hemorrhage (28,38).

Additional white matter abnormalities were detected by structural T1-weighted, T2-weighted, and fluid-attenuated inversion recovery MRI sequences. Five studies reported that a subset of survivors developed acute and/or persistent leukoencephalopathy (28,31–33,45), a condition associated with apparent white matter damage (ie, myelin damage) and defined by T2-weighted hyperintensity in white matter. Risk for leukoencephalopathy was highest among patients receiving more intensive therapy and higher doses of MTX (28,33).

Neurocognitive performance (ie, working memory and response inhibition) was associated with structural brain changes in ALL survivors. In particular, working memory performance correlated with white matter volume in the amygdala, thalamus, striatum, and corpus callosum, and response inhibition performance correlated with white matter volume in the frontal lobe (46). Moreover, reductions in total white matter volume correlated with deficits in academic performance, attention, and intelligence (43,44). Frontal and temporal lobe grey and white matter volumes were associated with math, reading, vocabulary, and memory span, and parietal lobe volume was associated with math and memory span (34). Higher plasma concentration of MTX was associated with poorer performance on metrics of cognitive flexibility, verbal fluency, spatial memory span, and numerical processing speed (6).

Diffusion MRI (White Matter Microstructure)

White matter microstructures were assessed in survivors using DTI and characterized by the degree of anisotropy and the directional orientation of water diffusivity (ie, metrics of white matter integrity). Statistically significant alterations in white matter integrity were noted among survivors of childhood ALL, which are summarized in Table 1 and Figure 3 (6,29–32,34,36,37,39,40,45). Survivors displayed impaired white matter

Table 1. Summary of brain imaging outcomes for survivors of childhood acute lymphoblastic leukemia

Reference	Study design	Population	Patient demographics; specific exposures	Modality; study objective	Neuroimaging changes; clinical outcomes
Badr et al. 2013 (28)	Observational cohort	25 ALL survivors No controls	Mean age at dx (SD) = 6.9 (3.04) years Mean age at evaluation (SD) = 12.9 (3.2) years No. (%) male subjects = 14 (56%) Specific exposures: IT MTX: n/a IV HDMTX: n/a IV HD cytarabine: n/a CNS+ status, n (%) = 3 (12%)	MRI (to identify neuroradiological abnormalities); to determine the prevalence and characteristics of late CNS damage by MRI and clinical examination in pediatric ALL	Neuroimaging changes: Using T1-weighted MRI images, abnormal brain findings were detected in 6 (24%) patients in the form of leukoencephalopathy (n = 2), brain atrophy (n = 2), infarct (n = 1), and hemorrhage (n = 1). Clinical outcomes: Patients treated with CRT (n = 4) and on higher risk protocols had an increased incidence of brain abnormalities.
Banerjee et al. 2019 (29)	Observational cross-sectional	212 ALL survivors (121 low risk, 91 standard/high risk) No controls	Mean age at dx (SD) = 6.7 (4.54) years Mean age at evaluation (SD) = 14.4 (4.79) years No. (%) male subjects = 107 (51%) Specific exposures, mean (SD): IT MTX = 15.33 (85.84) ml IV HDMTX = 203.42 (5.00) g/m^2 IV HD Cytarabine = n/a CNS+ status, n (%) = 32 (15.1%)	MRI, DTI; to investigate whether general anesthesia was associated with neurocognitive impairment and neuroimaging abnormalities in long-term survivors of pediatric ALL	Neuroimaging changes: Anesthesia was not associated with structural brain outcomes (MRI) or white matter diffusivity in the whole brain, frontal, or parietal lobes. Higher white matter diffusivity (ie, impaired integrity) in the corpus callosum was associated with higher propofol dose and longer anesthesia duration. Clinical outcomes: Processing speed was statistically significantly correlated with corpus callosum diffusivity. Neurocognitive impairment was associated with higher propofol cumulative dose, increased flurane exposure, and longer anesthesia duration.
Billiet et al. 2018 (30)	Observational cross-sectional	31 ALL survivors 35 controls	Mean age at dx = 6.4 years Mean age at evaluation = Not reported No. (%) Male subjects = 14 (45%) Survivors were enrolled on 2 similar treatment protocols.	MRI, DTI, rsfMRI; to examine associations between cognitive flexibility, resting state connectivity, and white matter diffusivity in ALL survivors	Neuroimaging changes: Survivors had lower functional connectivity between the default mode network and the inferior temporal gyrus (rsfMRI)

(continued)

Table 1. (continued)

Reference	Study design	Population	Patient demographics; specific exposures	Modality; study objective	Neuroimaging changes; clinical outcomes
			Specific exposures, mean (range): IT MTX: protocol 1 = 123.4 (86-228) mg; protocol 2 = 128.0 (100-192) mg IV HDMTX: protocol 1 = 15.8 (11-25) mg; protocol 2 = 19.3 (12-33) mg IV HD Cytarabine = n/a CNS+ status = n/a		and increased FA (DTI) in the left centrum semiovale. There were no volumetric differences. Clinical outcomes: Impaired cognitive flexibility in survivors was associated with altered FA in the left centrum semiovale.
Cheung et al. 2018 (31)	Observational cohort	235 ALL survivors (105 with MRI data) No controls	Mean age at dx (SD) = 6.7 (4.7) years Mean age at evaluation (SD) = 13.6 (4.6) years No. (%) male subjects with MRI data = 66 (48%) Specific exposures, mean (SD): IT MTX = 175.7 (54.0) mg IV HDMTX = 15.5 (5.1) g/m^2 IV HD Cytarabine = n/a CNS+ status, n (%) = 62 (26%)	DTI; to examine concentrations of cerebrospinal fluid (CSF) biomarkers of brain injury at ALL diagnosis and during cancer therapy and to evaluate associations with long-term neurocognitive, neuroimaging outcomes and genetic polymorphisms	Neuroimaging changes: Increases in GFAP, MBP, and total tau levels (from baseline through consolidation) were associated with a higher risk for leukoencephalopathy (determined using T2-weighted and T2 FLAIR MRI images) and higher apparent diffusion coefficient in frontal lobe white matter, 5 years after diagnosis. Clinical outcomes: Increases in total tau at consolidation were associated with poorer attention. Cerebral spinal fluid biomarkers may aid in identifying survivors at risk for poorer neurological outcomes.
Cheung et al. 2016 (32)	Observational cross-sectional	190 ALL survivors (51 with acute leukoencephalopathy, 139 without) No controls	ALL + leukoencephalopathy Mean age at dx (SD) = 7.1 (4.7) years Mean age at evaluation (SD) = 14.8 (4.5) years No. (%) Male subjects = 30 (59%) Specific exposures, mean (SD): IT MTX, No. of injections = 15.1 (4.1) IV HDMTX = 15.3 (4.5) g/m^2 IV HD Cytarabine =7.8 (0.8) g/m^2 CNS+ status = n/a ALL + no leukoencephalopathy Mean age at dx (SD) =5.7 (3.8) years	DTI; to examine associations between leukoencephalopathy, neurocognitive and neurobehavioral outcomes, and white matter integrity in ALL survivors	Neuroimaging outcomes: Survivors with a history of acute leukoencephalopathy (determined using T2-weighted and T2 FLAIR MRI images) had reduced white matter integrity in the frontostriatal tract (ie, lower FA, higher AD and RD). Clinical outcomes: Survivors with a history of acute leukoencephalopathy experienced greater neurobehavioral problems and cognitive impairment.

(continued)

Table 1. (continued)

Reference	Study design	Population	Patient demographics; specific exposures	Modality; study objective	Neuroimaging changes; clinical outcomes
			Mean age at evaluation (SD) = 13.3 (4.2) years No. (%) male subjects = 66 (48%) Specific exposures, mean (SD): IT MTX = 14.0 (3.9) g/m^2 IV HDMTX = 15.6 (7.3) g/m^2 IV HD Cytarabine = 8.9 (3.9) g/m^2 CNS+ status = n/a		Acute leukoencephalopathy during therapy predicted long-term neurocognitive problems and reduced white matter integrity in the frontal lobe, a region critical for higher-ordered cognitive processes.
Duffner et al. 2014 (33)	Observational cross-sectional	66 ALL survivors (59 with MRI data; 35 standard risk, 24 lesser risk) No controls	Standard risk group: Mean age at dx = 4.9 years Mean age at evaluation = 12.7 years No. (%) male subjects = 17 (49%) Lesser risk group: Mean age at dx = 4.1 years Mean age at evaluation = 11.8 years No. (%) male subjects = 15 (63%) Specific exposures: IT MTX = n/a IV HDMTX = n/a IV HD Cytarabine = n/a CNS+ status = n/a	MRI (to identify leukoencephalopathy); to compare neurocognitive and neuroradiologic outcomes between survivors treated with intense CNS directed therapy (SR) and those treated with fewer CNS-directed treatment days during intensive consolidation (LR)	Neuroimaging changes: Patients treated with more intensive therapy (SR) had increased prevalence of leukoencephalopathy identified at long-term follow-up (68% vs 22%), compared with patients with less intensive treatment. Clinical outcomes: Overall, survivors in both risk groups had statistically significant attention problems. Patients treated with more intensive therapy (SR) scored below average on more neurocognitive measures (82% vs 24%), compared with patients with less intensive treatment.
Edelmann et al. 2014 (34)	Observational cross-sectional	75 ALL survivors (36 chemotherapy-only, 39 CRT) 23 controls	ALL + chemotherapy: Mean age at dx (SD) = 9.97 (3.99) years Mean age at evaluation (SD) = 24.94 (3.58) years No. (%) male subjects = 21 (58%) Specific exposures, mean (SD): IT MTX = 163.4 (58.7) ml IV HDMTX = 20453 (3159) mg/mm^2 IV HD Cytarabine = 488.7 (177.7) ml CNS+ status, n (%) = 4 (11%) ALL + CRT: Mean age at dx (SD) = 2.81 (1.73) years	MRI, DTI; to compare neurocognitive function and brain morphology between long-term survivors of ALL treated with chemotherapy alone, those treated with CRT, and controls	Neuroimaging changes: Survivors of ALL, regardless of treatment, had reduced white matter volume in the frontal and temporal lobes, compared with controls. Survivors treated with chemotherapy had higher FA in white matter tracts within the left hemisphere, but not right, compared with controls. Clinical outcomes: ALL survivors also had impaired cognitive performance compared to population

(continued)

Table 1. (continued)

Reference	Study design	Population	Patient demographics; specific exposures	Modality; study objective	Neuroimaging changes; clinical outcomes
			Mean age at evaluation (SD) = 23.1 (3.44) years No. (%) male subjects = 18 (46%) Specific exposures, mean (SD): CRT = 20.0 (5.7) Gy IT MTX = 261.1 (116.7) ml IV HDMTX =5450 (3965) mg/mm^2 IV HD Cytarabine = 740.3 (274.6) ml CNS+ status, n (%) = 11 (31%)		norms, but ALL survivors treated with chemotherapy alone performed better than survivors treated with CRT. Neurocognitive performance was associated with white and grey matter volume in the frontal and temporal lobes.
Edelmann et al. 2013 (35)	Observational cross-sectional	38 ALL survivors (18 treated with dexamethasone, 20 treated with prednisone) No controls	ALL + dexamethasone: Median age at dx = 11. 8 years Median age at evaluation = 24.6 years No. (%) Male subjects = 12 (67%) Specific exposures, mean (range) IT MTX = 180 (132-264) ml IV HDMTX = 20478 (17352-25571) mg/m^2 IV HD Cytarabine = 540 (396-792) ml CNS+ status = n/a ALL + prednisone: Median age at dx = 8.7 years Median age at evaluation = 24.6 years No. (%) Male subjects = 10 (50%) Specific exposures, mean (range): IT MTX = 180 (156-264) ml IV HDMTX = 21030 (5207-25571) mg/m^2 IV HD Cytarabine = 540 (468-792) ml CNS+ status = n/a	Task-related fMRI; to compare neurocognitive outcomes and functional brain activity in ALL survivors treated with dexamethasone or prednisone	Neuroimaging changes: Dexamethasone treatment in ALL survivors was associated with decreased fMRI activity in the left retrosplenial brain region. Story memory was associated with altered activation in the left inferior frontal-temporal brain regions. Clinical outcomes: Survivors treated with dexamethasone had lower memory performance, compared to survivors treated only with prednisone.
ElAlfy et al. 2014 (36)	Observational cross-sectional	62 ALL survivors (3 separate treatment protocols: n = 30 CCG protocol, n = 21 BFM 90 protocol, n = 11 BFM 83 protocol) 60 controls	CCG standard risk protocol group Mean age at dx (SD) = 5.27 (2.38) years Mean age at evaluation (SD) = 8.40 (2.71) years No. (%) male subjects = 16 (53%) BFM 90 standard risk protocol group Mean age at dx (SD) = 5.6 (3.19) years	DTI; to assess the associations between neurocognitive outcomes and white matter integrity in ALL survivors treated on 3 separate treatment protocols (CCG, BFM 90, BFM 83)	Neuroimaging changes: ALL survivors treated on more intensive therapy protocols had decreased FA (ie, impaired white matter integrity) in the frontal lobe compared with patients treated on less intensive protocols and controls.

(continued)

Table 1. (continued)

Reference	Study design	Population	Patient demographics; specific exposures	Modality; study objective	Neuroimaging changes; clinical outcomes
			Mean age at evaluation (SD) = 12.39 (2.53) years No. (%) male subjects = 10 (48%) BFM 83 standard risk-low protocol group Mean age at dx (SD) = 6.33 (3.80) years Mean age at evaluation (SD) = 14.44 (2.12) years No. (%) male subjects = 7 (64%) Specific exposures: IT MTX = n/a IV HDMTX = n/a IV HD Cytarabine = n/a CNS+ status = n/a		Clinical outcomes: ALL survivors treated on more intensive therapy protocols also had worse neurocognitive performance compared with patients treated on less intensive protocols and controls.
Fellah et al. 2019 (7)	Observational cohort	165 ALL survivors No controls	Mean age at dx (SD) = 4.7 (4.4) years Mean age at evaluation (SD) = 14.4 (4.7) years No. (%) male subjects = 85 (51.5%) Specific exposures, mean (SD): IT MTX = 168.1 (56.3) ml IV HDMTX = 13.0 (7.4) g/m^2 (low risk); 20.0 (4.5) g/m^2 (standard risk) IV HD Cytarabine = n/a CNS+ status = n/a	Task-related fMRI; to examine neurocognitive function (CPT: executive function, ANT: attention) and functional MRI in childhood ALL survivors	Neuroimaging changes: Regional brain activation was lower in survivors diagnosed at younger ages. Survivors had lower brain activation in the bilateral parietal and temporal lobes during the continuous performance task (CPT) and lower brain activation in the left parietal and right hippocampus during the attention network task (ANT). Treatment exposure was associated with fMRI activity. Survivors with higher serum MTX exposure had lower activation in the right temporal and bilateral frontal and parietal lobes during the CPT and increased activation in the ventral frontal, insula, caudate, and anterior cingulate during the ANT. Clinical outcomes: Survivors had impaired attention and executive function, which was associated with increased treatment

(continued)

Table 1. (continued)

Reference	Study design	Population	Patient demographics; specific exposures	Modality; study objective	Neuroimaging changes; clinical outcomes
					intensity and younger age at diagnosis.
Genschaft et al. 2013 (37)	Observational cross-sectional	27 ALL survivors 27 controls	Mean age at dx (SD) = 5.6 (2.5) years Mean age at evaluation (SD) = 17.9 (2.4) years No. (%) male subjects = 13 (48%) Specific exposures: IT MTX = n/a IV HDMTX = n/a IV HD Cytarabine = n/a CNS+ status = n/a	MRI, DTI; to examine brain morphology (voxel-based morphometry, DTI) and neurocognitive outcomes in survivors of childhood ALL	Neuroimaging changes: Survivors had statistically significant reductions in volume of the bilateral hippocampi and left nucleus accumbens, thalamus, amygdala, calcarine gyrus, lingual gyri, and precuneus. There were no differences in white matter pathology as measured by DTI. Clinical outcomes: Survivors were impaired on hippocampal-dependent memory tasks compared with controls.
Kalafatçılar et al. 2014 (38)	Observational cross-sectional	44 ALL survivors 14 sibling controls	Mean age at dx = 5.5 years Mean age at evaluation = 16.4 years No. (%) male subjects = 23 (52%) Specific exposures: IT MTX = n/a IV HDMTX = n/a IV HD Cytarabine = n/a CNS+ status = n/a	MRI (to identify neuroradiological abnormalities); to identify neuropsychological late effects using metrics of neurocognitive, behavioral, and MRI outcomes	Neuroimaging changes: A subset of patients (8/44; 18.2%) had cranial MRI abnormalities, most commonly, cerebral microangiopathy (n = 3). Clinical outcomes: The majority of survivors (70%) had impaired neurocognitive performance. Patients aged older than 6 years at time of diagnosis were found to have more psychological problems and higher rates of unhealthy behavior (smoking and alcohol consumption).
Kesler et al. 2016 (39)	Observational cross-sectional	31 ALL survivors 39 controls	Mean age at dx (SD) = 5.4 (3.7) years Mean age at evaluation (SD) = 11 (3.4) years No. (%) male subjects = 14 (45%) Specific exposures: IT MTX = n/a IV HDMTX = n/a IV HD Cytarabine = n/a CNS+ status = n/a	DTI; to examine the organization of white matter connectome in survivors of ALL	Neuroimaging changes: ALL survivors had lower small-worldness and lower network clustering (ie, decreased connectivity of neighboring brain regions). Survivors also had altered clustered connectivity in the parietal, frontal, hippocampal, amygdalar,

(continued)

Table 1. (continued)

Reference	Study design	Population	Patient demographics; specific exposures	Modality; study objective	Neuroimaging changes; clinical outcomes
					thalamic, and occipital regions. Clinical outcomes: Reductions in information processing efficiency, cognitive reserve, and network connectivity may contribute to the cognitive deficits observed in ALL survivors.
Kesler et al. 2018 (40)	Observational cross-sectional	161 ALL survivors (100 nonimpaired, 61 impaired executive function)	Nonimpaired group: Mean age at dx (SD) = 7.08 (4.6) years Mean age at evaluation (SD) = 14.87 (4.9) years No. (%) male subjects = 40 (40%) Impaired group: Mean age at dx (SD) = 6.47 (4.1) years Mean age at evaluation (SD) = 14.23 (4.4) years No. (%) male subjects = 39 (64%) Specific exposures, mean (SD): IT MTX = 14.43 (4.1) ml (nonimpaired); 14.77 (4.0) ml (impaired) IV HDMTX = n/a IV HD Cytarabine = n/a CNS+ status = n/a	rsfMRI, DTI; to investigate functional and microstructural connectome organization between ALL survivors with or without executive dysfunction at long-term follow-up	Neuroimaging changes: Survivors with impaired executive function displayed lower global efficiency (ie, reduced network integration and information exchange) as measured by microstructural and functional connectomes, than nonimpaired survivors. Patients receiving more intensive therapy (ie, standard or high risk, increased intrathecal MTX administration) had the lowest network efficiencies. Impaired survivors showed hyperconnectivity in brain regions involving sensorimotor, visual, and auditory processing and had poor separation between sensorimotor, executive function, attention, salience, and default mode networks via resting state fMRI. Clinical outcomes: Disruptions in connectome organizations are consistent with patterns of delayed neurodevelopment, which may be associated with reduced flexibility and resilience of

(continued)

Table 1. (continued)

Reference	Study design	Population	Patient demographics; specific exposures	Modality; study objective	Neuroimaging changes; clinical outcomes
					brain networks in ALL survivors.
Kesler et al. 2010 (41)	Observational cross-sectional	28 ALL survivors 31 controls	Mean age at dx (SD) = not reported Mean age at evaluation (SD) = 12.0 (4.6) years No. (%) male subjects =16 (56%) Specific exposures: IT MTX: n/a IV HDMTX: n/a IV HD Cytarabine: n/a CNS+ status: n/a	MRI; to examine associations between white and grey matter volume and cognitive outcomes in ALL survivors and to investigate maternal education and its relationship with white and grey matter volume in ALL survivors	Neuroimaging changes: Survivors had lower total white matter volume and displayed statistically significant white matter volume reductions in the left corpus callosum, right caudate, bilateral thalamus, bilateral superior fronto-occipital fasciculus, and fornix, which corresponded with impairments in cognitive performance. Clinical outcomes: Reduced white matter corresponded with cognitive impairments in ALL survivors. Maternal education was inversely correlated with global and regional white matter volumes and positively correlated with gray matter volume.
Krull et al. 2016 (6)	Observational cohort	218 ALL survivors	Mean age at dx (SD) = 6.6 (4.5) years Mean age at evaluation (SD) = 13.8 (4.8) years No. (%) male subjects =112 (51%) Specific exposures: mean (SD) IT MTX = 170.3 (55.2) ml IV HDMTX = 15.7(6.6) g/m^2 IV HD Cytarabine = 8.4 (3.0) g/m^2 CNS+ status = n/a	MRI, DTI, task-related fMRI; to examine the relationship between methotrexate pharmacodynamics, neuroimaging, and neurocognitive outcomes in ALL survivors	Neuroimaging changes: Higher plasma concentration of MTX was associated with increased brain fMRI activity (ie, increased activity in the frontal and anterior cingulate cortices, the caudate nuclei, and putamen during an attention network task), thicker cortices in the dorsal lateral prefrontal brain regions (MRI) and reduced white matter integrity in the frontostriatal tract (DTI). Clinical outcomes: A higher plasma concentration of MTX was associated with poorer executive function.

(continued)

Table 1. (continued)

Reference	Study design	Population	Patient demographics; specific exposures	Modality; study objective	Neuroimaging changes; clinical outcomes
Phillips et al. 2019 (42)	Observational cross-sectional	218 ALL survivors 82 controls	Median age at dx = 6.8 years Median age at evaluation = 14.5 years No. (%) male subjects = 107 (49%) Specific exposures: IT MTX = n/a IV HDMTX = n/a IV HD Cytarabine = n/a CNS+ status = n/a	MRI; to investigate the association between treatment exposures and brain morphology in childhood ALL survivors, with a focus on brain regions with high concentrations of glucocorticoid receptors	Neuroimaging changes: Survivors displayed smaller volumes in the bilateral cerebellum, hippocampus, temporal lobe regions, frontal lobe, and parietal lobe regions including the precuneus. Survivors had thinner cortices in the parahippocampal, fusiform gyrus, caudal middle frontal, superior frontal, rostral middle frontal, rostral anterior cingulate, and precuneus regions. Higher dexamethasone was associated greater cortical thinning in the frontal, temporal, and parietal lobes, particularly among female survivors who displayed a different pattern of cortical thinning compared with male survivors. Clinical outcomes: Survivors show changes in brain regions that are high in glucocorticoid receptors following therapy.
Reddick et al. 2006 (43)	Observational cross-sectional	112 ALL survivors (84 chemotherapy alone, 28 chemotherapy + CRT) 33 sibling controls	ALL + chemotherapy Mean age at dx (SD) = 4.5 (2.6) years Mean age at evaluation (SD) = 9.8 (3.1) years No. (%) male subjects = 47 (56%) ALL + chemotherapy + CRT Mean age at dx (SD) = 3.1 (2.3) years Mean age at evaluation (SD) = 11.1 (2.6) years No. (%) male subjects = 16 (57%) Specific exposures: IT MTX: n/a IV HDMTX: n/a	MRI; to examine associations between white matter volume and neurocognitive performance in survivors of ALL	Neuroimaging changes: Survivors, regardless of treatment, had reduced white matter volume and impaired attention compared with controls. Reduced white matter volumes were associated with greater deficits in cognitive domains of attention, intelligence, and academic achievement. Clinical outcomes: Deficits in white matter volume and cognitive performance

(continued)

Table 1. (continued)

Reference	Study design	Population	Patient demographics; specific exposures	Modality; study objective	Neuroimaging changes; clinical outcomes
			IV HD Cytarabine: n/a CNS+ status: n/a		were present in all survivors but was most pronounced among survivors treated with CRT.
Reddick et al. 2014 (44)	Observational cross-sectional	199 ALL survivors 184 brain tumor survivors 67 sibling controls	ALL survivors: Mean age at dx (SD) = 4.7 (2.7) years Mean age at evaluation (SD) = 12.4 (3.3) years No. (%) male subjects = 112 (56%) Brain tumor survivors: Mean age at dx (SD) = 6.5 (3.6) years Mean age at evaluation (SD) = 11.9 (3.4) years No. (%) male subjects = 101 (55%) Specific exposures: IT MTX = n/a IV HDMTX = n/a IV HD Cytarabine = n/a CNS+ status = n/a	MRI; to investigate the associations between white matter volume, treatment factors, and neurocognitive performance in ALL survivors and brain tumor survivors	Neuroimaging changes: Survivors of ALL had decreased cerebral white matter volumes compared with sibling controls. Increased CNS treatment intensity, younger age at treatment, and greater time since treatment were statistically significantly associated with lower total white matter volume. Clinical outcomes: Reductions in white matter volume correlated with deficits in academic performance, attention, and intelligence.
Sabin et al. 2018 (45)	Observational cross-sectional	173 ALL survivors	Mean age at dx (SD) = 6.7 (4.3) years Mean age at evaluation (SD) = 14.4 (4.6) years No. (%) male subjects = 89 (51%) Specific exposures, mean (SD): IT MTX, No. of injections: 14.4 (4.0) IV HDMTX 15.4 (6.7) g/m^2 IV HD Cytarabine = 8.5 (3.5) g/m^2 CNS+ status = n/a	DTI; to conduct a longitudinal assessment of leukoencephalopathy and examine the association with white matter integrity and neurocognitive performance at long-term follow-up in ALL survivors	Neuroimaging changes: A subset of survivors (30%) developed acute leukoencephalopathy during therapy, and 78.8% of those survivors continued to display leukoencephalopathy at long-term follow-up. Leukoencephalopathy was associated with impaired white matter integrity in the corona radiata, superior longitudinal fasciculi, and superior fronto-occipital fasciculi. Mean diffusivity in the genu of the corpus callosum, corona radiata, and superior fronto-occipital fasciculi correlated with neurocognitive impairment. Clinical outcomes: Leukoencephalopathy

(continued)

Table 1. (continued)

Reference	Study design	Population	Patient demographics; specific exposures	Modality; study objective	Neuroimaging changes; clinical outcomes
					during active therapy was associated with poorer neurocognitive performance at long-term follow-up. Diffusion tensor imaging is a sensitive measure to detect clinically relevant white matter abnormalities in survivors.
Van der Plas et al. 2017 (46)	Observational cross-sectional	23 ALL survivors 21 controls	Mean age at dx (SD) = 4.4 (1.8) years Mean age at evaluation (SD) = 14.4 (2.2) years No. (%) male subjects = 26 (100%) Specific exposures: IT MTX = n/a IV HDMTX = n/a IV HD Cytarabine = n/a CNS+ status = n/a	MRI; to explore variations in brain volume and neurocognitive performance among ALL survivors	Neuroimaging changes: Survivors had reduced white matter volume in the frontal and parietal regions and reduced grey matter volume in the temporal and occipital regions. Survivors also had reduced subcortical white matter volume in the corpus callosum, bilateral anterior corona radiata, right superior corona radiata, bilateral posterior corona radiata, left anterior limb on the internal capsule, left cingulum cingulate gyrus, and left superior longitudinal fasciculus. Clinical outcomes: Working memory performance correlated with volume in the amygdala, thalamus, striatum, and corpus callosum. Response inhibition correlated with white matter volume in the frontal lobe.
Zając-Spychała et al. 2017 (47)	Observational cross-sectional	33 ALL survivors (22 chemotherapy-only, 11 CRT) 12 controls	ALL + HDMTX Median age at dx = 5.2 years Median age at evaluation = 12.1 years No. (%) male subjects = 11 (50%) ALL + chemotherapy + CRT Median age at dx = 4.9 years Median age at evaluation = 11.6 years No. (%) male subjects = 6 (55%)	MRI; to assess long-term brain structure and cognitive function in ALL survivors treated with high-dose methotrexate chemotherapy or CRT	Neuroimaging changes: Survivors treated with high-dose chemotherapy had reduced caudate nucleus volume, which correlated with impaired verbal fluency. Clinical outcomes: Survivors treated with the addition of CRT had greater cognitive

(continued)

Table 1. (continued)

Reference	Study design	Population	Patient demographics; specific exposures	Modality; study objective	Neuroimaging changes; clinical outcomes
			Specific exposures IT MTX = n/a IV HDMTX = n/a IV HD Cytarabine = n/a CNS+ status = n/a		impairments compared with survivors who received high-dose MTX.
Zając-Spychała et al. 2018 (48)	Observational cross-sectional	78 ALL survivors (31 Intermediate-MTX, 17 HD-MTX, 30 CRT) 23 controls	ALL + intermediate MTX Median age at dx = 6.2 years Median age at evaluation = 11.8 years No. (%) male subjects = 19 (61%) ALL + HDMTX Median age at dx 8.5 years Median age at evaluation =11.2 years No. (%) male subjects =10 (59%) ALL + chemotherapy + CRT Median age at dx =6 years Median age at evaluation =12 years No. (%) male subjects =14 (61%) Specific exposures: IT MTX = n/a IV HDMTX = n/a IV HD Cytarabine = n/a CNS+ status = n/a	MRI; to evaluate brain structure in survivors of ALL treated with intermediate or high-dose chemotherapy or CRT	Neuroimaging changes: Survivors of ALL treated with intermediate or high-dose chemotherapy did not display any volumetric differences compared with controls. Survivors treated with CRT had statistically significant volumetric reductions compared with controls and survivors treated with chemotherapy alone. Clinical outcomes: Survivors of ALL treated with intermediate or high-dose chemotherapy had impaired cognitive performance compared with controls and survivors treated with chemotherapy alone. Survivors treated with CRT had poorer cognitive performance.

[a]AD = axial diffusivity; ALL = acute lymphoblastic leukemia; ANT = attention network task; BFM = Berlin-Frankfurt-Münster; CCG = Children's Cancer Group; CNS = central nervous system; CPT = continuous performance task; CRT = cranial radiation therapy; CSF = cerebrospinal fluid; DTI = diffusion tensor imaging; dx = diagnosis; FA = fractional anisotropy; FLAIR = fluid-attenuated inversion recovery; fMRI = functional magnetic resonance imaging; GFAP = glial fibrillary acidic protein; HD = high dose; HDMTX = high dose methotrexate; HR = high risk; IT = intrathecal; IV = intravenous; LR = low risk; MBP = myelin basic protein; MRI = magnetic resonance imaging; MTX = methotrexate; RD = radial diffusivity; rsfMRI = resting state functional magnetic resonance imaging; SR = standard risk.

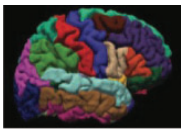

Altered Brain Structure

Grey matter volume reductions in frontal, parietal, temporal, and occipital lobes including the left nucleus accumbens, thalamus, amygdala, calcarine gyrus, caudate nucleus, lingual gyri, precuneus, bilateral hippocampi, and hippocampal subregions.

White matter volume reductions in the frontal, temporal, and parietal regions, subcortical regions including left corpus callosum, caudate nucleus, bilateral thalamus, and bilateral superior fronto-occipital fasciculus.

Cortical thinning in the parahippocampal, fusiform gyrus, caudal middle frontal, superior frontal, rostral middle frontal, rostral anterior cingulate, and precuneus regions.

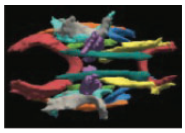

Impaired WM Integrity

White matter integrity deficits in the fronto striatal tract, frontal lobe, corpus callosum, left centrum semiovale, and left hemisphere.

Leukoencephalopathy was associated with impairment white matter integrity in the fronto striatal tract. Persistent leukoencephalopathy was associated with impaired integrity in the corona radiata, superior longitudinal fasciculi, and superior fronto-occipital fasciculi.

Altered white matter connectivity in the parietal, frontal, hippocampal, amygdala, thalamic, and occipital regions.

Reduced network clustering and small-worldness (ie decreased connectivity of neighboring brain regions) and reduced global efficiency (ie reduced network integration and information exchange) based on functional connectomes.

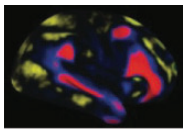

Altered Functional Connectivity

Reduced resting state connectivity between the default mode network and inferior temporal gyrus.

Survivors with executive dysfunction had lower global efficiency in functional connectome organization.

Survivors with executive dysfunction had hyperconnectivity in sensorimotor, visual, and auditory processing brain regions. They also had poor network separation between sensorimotor, executive function/attention, salience, and default mode networks.

Reduced BOLD signaling in the bilateral parietal and temporal lobes during a sustained attention task and reduced BOLD signaling in the left parietal and right hippocampus during an attention network task.

Figure 3. Summary of MRI-related outcomes in long-term survivors of acute lymphoblastic leukemia. BOLD = blood-oxygen-level-dependent; MRI = magnetic resonance imaging; WM = white matter.

integrity (ie, decreased FA, increased directional diffusivity) in the frontostriatal tracts, frontal lobe, corpus callosum, and other white matter fiber tracts (6,30,32,34,36). Moreover, higher plasma concentration of MTX during therapy was associated with impaired white matter integrity in the frontostriatal tracts and executive dysfunction (6). Only 1 study did not observe any differences in white matter pathology (37).

Connectome-based analysis of diffusion-weighted imaging revealed statistically significant alterations in microstructural white matter connectivity and network clustering in ALL survivors. Survivors had lower small-worldness and lower network clustering (ie, decreased connectivity of neighboring brain regions), which corresponded with impaired neurocognitive performance. Survivors also had altered cluster connectivity patterns (39). Survivors with impaired executive function displayed lower global network efficiency (ie, reduced network integration and information exchange) between white matter microstructures than survivors without executive dysfunction. In addition, survivors who received more intensive therapy (ie, standard or high risk, increased intrathecal MTX administration) had the lowest network efficiencies (40).

Apparent white matter damage was also reflected in diffusion measures of white matter integrity. Acute leukoencephalopathy was associated with long-term reductions in white matter integrity within the frontostriatal tracts (32). Persistent leukoencephalopathy was also associated with impaired white matter integrity in several different white matter tracts. Neurocognitive impairments at long-term follow-up correlated with the mean diffusivity of white matter tracts in survivors with persistent leukoencephalopathy. Moreover, the number of intrathecal administrations of MTX, hydrocortisone, and cytarabine was associated with higher mean diffusivity (ie, impaired white matter integrity) in several white matter tracts among survivors with persistent leukoencephalopathy (45).

The association of cerebrospinal fluid biomarkers of CNS injury and white matter integrity was also investigated in long-term ALL survivors. Increases in glial fibrillary acidic protein, myelin basic protein, and total tau levels from baseline through consolidation were associated with a higher risk for leukoencephalopathy, increased diffusivity in white matter in the frontal lobe, and greater neurocognitive impairments (31). The effects of anesthesia exposure on white matter integrity was also evaluated in ALL survivors. Higher doses of propofol and longer duration of anesthesia exposure was associated with attention deficits and increased diffusivity (ie, impaired white matter integrity) in the corpus callosum, a region critical for interhemispheric communication (29).

Functional MRI

Functional characteristics of the brain were measured using resting state and task-based fMRI, and the findings were summarized in Table 1 and Figure 3 (6,7,30,35,40). For resting state fMRI, survivors displayed lower functional brain connectivity between the default mode network and the inferior temporal gyrus (30). Survivors with impaired executive function had lower global efficiency (ie, reduced neighboring connections) in functional connectome organization. Impaired survivors also showed hyperconnectivity during resting state in brain regions involving sensorimotor, visual, and auditory processing and had poor separation between different brain networks (40).

For task-based fMRI, survivors had lower brain activation (ie, reduced BOLD signaling) in the bilateral parietal and temporal lobes during the continuous performance task (CPT), a metric of sustained attention, and lower brain activation in the left parietal and right hippocampus during an attention network task (ANT), a metric of attention and executive function as defined

by attentional arousal, spatial orientation, and cognitive flexibility (7). Survivors with higher serum MTX exposure had lower activation in the right temporal and bilateral frontal and parietal lobes during the CPT, and increased activation in the ventral frontal, insula, caudate, and anterior cingulate during the ANT (7). In a separate study, higher plasma concentrations of MTX were also associated with increased brain activity in the frontal and anterior cingulate cortices, the caudate nuclei, and putamen during the ANT (6). Younger age at diagnosis was associated with lower brain activation during the CPT and ANT (7). Furthermore, dexamethasone treatment was associated with increased memory problems and decreased fMRI activity in the left retrosplenial brain region while processing novel words compared to survivors treated with prednisone. Story memory was associated with altered activation in the left inferior frontal-temporal brain regions in survivors treated with dexamethasone (35).

Discussion

Brain Development in Pediatric ALL Survivors

Widespread alterations in brain anatomy and function were observed in long-term survivors of pediatric leukemia treated on chemotherapy-only protocols. The findings revealed that chemotherapy has a direct impact on brain anatomy, white matter integrity, and functional activation, particularly in the frontal lobe, hippocampus, and other regions involved in learning, memory, and executive function. Connectome-based analyses, derived from resting state fMRI and DTI, revealed lower network clustering, lower global efficiency, reduced network integration, and reduced information processing in ALL survivors. These combined findings suggest that the neuroanatomical structures are altered in survivors and the connections between them are disrupted. Disruptions in neural network communication and regional connectivity likely contribute, at least in part, to the neurocognitive late effects (ie, impaired attention, executive function, and processing speed) observed in survivors of childhood ALL.

It is important to note that many of these changes in brain anatomy and function are observed early in the years following chemotherapy (within 5-10 years), which suggests that chemotherapy-induced neurotoxicity progresses rapidly and must be intervened in a timely manner to mitigate long-term side effects. Although the majority of chemotherapy agents do not cross the BBB, genetic variability in BBB transporters can modify or increase the amount of neurotoxicity agents that enter the brain, potentially reducing the integrity of the barrier (49). Additionally, chemotherapy can lead to apoptosis and reduced cell division in the brain, which are processes that directly impact brain development and function (50). Chemotherapy may also inhibit brain development and worsen neurocognitive deficits through DNA damage induced by increased oxidative stress (51). Chemotherapy is also associated with shorter telomere length (52,53), suggesting that accelerating neural aging may occur in survivors who received chemotherapy (54). Cytokine dysregulation can also occur during chemotherapy and is associated with neural inflammation and DNA damage (55). Dysregulation of proinflammatory cytokines is also present in neurodegenerative disorders associated with accelerated aging and severe cognitive impairments such as Alzheimer disease (56). These findings may again suggest that survivors are at risk for accelerated neural decline and cognitive deficits. The neurotoxic effects of chemotherapy can also be mediated by differences in sex hormones, such as variations in levels of estrogen or testosterone, which can serve as neuroprotective agents against chemotherapy (57,58). Estrogen has also been shown to have neuroprotective properties for preserving telomere length (59). These findings suggest that patients with reduced estrogen or testosterone may be more susceptible to the chemotherapy-related neurotoxicity. Moreover, based on the findings in this review, female survivors displayed greater structural differences (reduced volume, greater cortical thinning) compared with male survivors (42), demonstrating that hormonal differences can affect the degree of neurotoxic damage incurred during treatment. Although some of the neuroimaging studies in this review included ALL survivors treated on sex-specific protocols (ie, males received 6 more months of treatment than females), these differences are negligible as males typically received maintenance drugs and low doses of oral MTX, which are not commonly associated with neurotoxicity. Moreover, all of the observed sex-based differences in neuroimaging outcomes were reported exclusively among females, further suggesting that sex and hormonal differences may be playing a key role in long-term neural development. Overall, chemotherapy-induced brain changes are multifactorial in nature and will require a multidisciplinary approach, utilizing multiple neuroimaging techniques, to fully understand the mechanisms underlying neurotoxicity in long-term survivors of ALL.

Another potential mechanism of chemotherapy-induced neurotoxicity involves impaired neurogenesis (ie, the generation of new neurons). Chemotherapy disrupts the proliferation of neurogenesis in the dentate gyrus of the hippocampus, a brain region involved in learning and memory (60). Preclinical models have also demonstrated that chemotherapy is associated with a statistically significant decline in neurogenesis and impaired cognitive function, particularly for hippocampal-dependent memory functions (11). These findings may partially explain the mechanism underlying the smaller hippocampal volumes observed in long-term survivors of ALL, but the exact mechanism between hippocampal volume and neurogenesis has not yet been established. However, the results from this review revealed that survivors had statistically significant reductions in hippocampal volume (37,42) and impaired performance on hippocampal-dependent memory tasks (37), which is consistent with the mechanism of impaired hippocampal neurogenesis and cognitive dysfunction. Connectome-based analyses using DTI also revealed altered clustered connectivity in the hippocampus, among other regions (39). Future studies should use high-resolution MRI to segment subregions of the hippocampus and use in vivo magnetic resonance spectroscopy (MRS) and chemical exchange saturation transfer (CEST)–based imaging to assess the molecular composition of the brain to better understand the role of hippocampal neurogenesis and how it may be impacted in long-term ALL survivors.

Although chemotherapy treatment exposures are acute, they are still administered during a period of rapid brain development which has long-term implications on brain function and cognitive abilities. Longitudinal MRI investigations of brain development during childhood and adolescence have shown complex patterns of regionally specific development in brain architecture (ie, volume, cortical thickness, and surface area), which are age-related and differ by sex (61–63). These developmental brain changes continue to occur throughout early adulthood until the brain reaches full maturation (64). Studies have demonstrated that white matter maturation develops more

slowly in frontotemporal regions during childhood and adolescence (65), which may suggest that these white matter regions are most vulnerable to the neurotoxic effects of CNS-directed chemotherapy because of their lack of mature myelin development. Consistent with these findings, long-term survivors of ALL treated with chemotherapy during childhood and adolescence also displayed damages to white matter integrity in these regions (ie, frontostriatal tracts), which was accompanied by executive dysfunction (6). Damages to white matter integrity may lead to further disruptions in network connectivity patterns and reduce information processing efficiency. Future studies should employ multiple MRI techniques to better understand how white matter alterations are associated with changes in brain architecture and function. Brain-related changes should be closely monitored throughout therapy and during long-term follow-up to identify longitudinal changes that may be associated with treatment exposures and neurotoxicity. To potentially mitigate the harmful effects of chemotherapy on brain structure and function, brain stimulation techniques such as transcranial direct current stimulation, transcranial alternative current stimulation, and photo-biomodulation can be used to stimulate different neural networks, at different frequencies, to enhance or inhibit brain activity. Stimulation of frontal lobe networks in ALL survivors may be particularly beneficial given that these survivors displayed reduced frontal lobe volume, altered frontal lobe activity during attention-related tasks, altered frontal lobe connectivity with poorer network efficiencies, and reduced white matter integrity in the frontostriatal tracts, particularly among survivors who developed acute leukoencephalopathy during treatment. These stimulation techniques may also improve the neurocognitive deficits observed in ALL survivors, as they have well-documented deficits in attention, executive function, and processing speed, which are cognitive processes mediated by frontal lobe networks (6,7).

Leukoencephalopathy

Acute leukoencephalopathy occurs in a subset of ALL patients receiving treatment. Patients with acute leukoencephalopathy can be symptomatic or asymptomatic, which can sometimes make it difficult to detect without serial MRI monitoring. For some patients, leukoencephalopathy is associated with stroke-like symptoms including seizures, dysphasia, and altered mental status (66,67). Regardless of whether patients experience overt symptoms related to leukoencephalopathy, white matter damage can still occur. As observed in this review, risk for leukoencephalopathy was highest among survivors who received more intensive therapy and higher doses of MTX (28,33). Leukoencephalopathy during treatment was associated with long-term impairments in white matter integrity, particularly in the frontostriatal tracts, a white matter fiber bundle critically involved in higher-ordered cognitive processes (32). Survivors with persistent leukoencephalopathy (from active therapy to long-term follow-up) experienced greater neurocognitive deficits and had reduced white matter integrity in the corpus callosum, corona radiata, superior longitudinal fasciculi, and superior fronto-occipital fasciculi, reflecting widespread alterations in white matter networks. These findings demonstrate that acute and chronic disruptions to white matter integrity (ie, myelin damage) can have a lasting impact on brain function and cognitive development. Overall, patients with acute or persistent leukoencephalopathy have greater neuroanatomical changes, increased neurocognitive impairment, and reduced white matter integrity at long-term follow-up. Although all patients receiving chemotherapy are at risk for developing neurocognitive deficits and impaired brain function, patients who develop leukoencephalopathy during therapy may be at greater risk and require a modified or earlier intervention to help mitigate long-term neurocognitive and brain dysfunction.

Inflammation biomarkers collected from the CSF during therapy may also be particularly useful for predicting acute leukoencephalopathy and long-term impairments in neurocognitive abilities and brain function. Increases in glial fibrillary acidic protein, myelin basic protein, and total tau levels from baseline through consolidation were associated with a higher risk for leukoencephalopathy and increased diffusivity (ie, white matter damage) in the frontal lobe (31). These findings demonstrate that biomarkers of inflammation collected during treatment could be useful in predicting acute, as well as later, changes in brain development and cognitive ability. By assessing biomarkers associated with brain function, early identification of patients at higher risk for developing leukoencephalopathy can be detected, and early interventions can be applied.

Treatment Factors Impact Brain Development

Treatment factors also played an influential role in brain development in survivors. Survivors treated with more intensive therapy (ie, standard or high risk compared with low risk) had lower network efficiency between brain regions, had altered brain structure and function, and displayed greater neurocognitive impairments. The number of intrathecal administrations of MTX, hydrocortisone, cytarabine, and dexamethasone was positively correlated with impaired white matter integrity in survivors with persistent leukoencephalopathy at long-term follow-up (45). The effect of CNS disease status was only reported for a subset of studies (4 of 23; 17.4%), and it was not reported to be associated with any neuroimaging outcomes. However, larger research investigations with adequate power are warranted to determine the extent to which CNS disease status may affect long-term brain development and function in ALL survivors. CNS disease will be an important factor to consider in future neuroimaging investigations given emerging evidence that suggests CNS changes may occur prior to treatment and are related to neuroinflammation (31). Additionally, higher dexamethasone exposure was associated with increased cortical thinning, particularly among female survivors (42). This suggests that differences in sex hormones (ie, endocrine system) may mediate the effect of chemotherapy on brain structure. Dexamethasone exposure also altered BOLD signaling, which corresponded with memory deficits (35). No associations were observed between dexamethasone exposure and hippocampal volume (42), despite previous literature reporting hippocampi atrophy in individuals with prolonged exposure to glucocorticoids (68). However, the effects of steroid use (ie, dexamethasone, prednisone) on brain structure in ALL survivors have only been investigated in a single-institution study, and additional research studies are warranted. Overall, these findings highlight the deleterious effects of dexamethasone exposure on brain structure (ie, reduced volume, increased cortical thinning) and function (ie, altered hemodynamic responses during a memory-related cognitive task), indicating that dexamethasone exposure should be reduced when possible.

The effect of anesthesia was also investigated as a treatment factor but yielded no effect on the structural properties of the

brain, as assessed using T1-weighted MRI images. However, anesthesia exposure did have an impact neurocognitive function and white matter integrity in ALL survivors. Specifically, higher doses of propofol and increased duration of anesthesia exposure were associated with attention deficits and increased diffusivity in the corpus callosum, a region critical for interhemispheric communication (29). As such, exposure to anesthesia should be limited as much as possible to prevent long-term deficits in white matter integrity and neurocognitive late effects.

We acknowledge a few limitations common to systematic reviews and the nature of synthesizing large datasets. To reduce these limitations, the PRISMA guidelines were adhered. Risk for selection bias and low participation rates was also noted for a few studies, but the majority of studies did not exhibit a risk of bias. Studies that examined the molecular properties of the brain using MRS- or CEST-based imaging were not included in this review, nor were other non-MRI modalities such as magnetoencephalography, electroencephalography (EEG), and functional near-infrared spectroscopy (fNIRS), which may have provided additional studies and further insight into brain function following chemotherapy, particularly for understanding the temporal and electrophysiological properties of the brain. Myelin water imaging was also reported as an outcome for one of the studies (30), but these results were not considered given the scope of this review.

Discussion

The neurotoxic effects of cancer treatment are reduced in the absence of cranial radiation, but survivors treated with chemotherapy still display some deficits in brain structure and function, which may contribute to the neurocognitive late effects observed in long-term survivors. Importantly, acute neurotoxicity that occurs during chemotherapy can have a lasting impact on brain development long after treatment has subsided. For these reasons, long-term survivors of childhood ALL should be closely monitored for neurocognitive deficits and corresponding brain dysfunction. Investigators should use domain-specific neurocognitive testing, rather than global cognitive measures, to monitor changes in cognitive abilities among survivors. Studies that investigate neurocognitive late effects in survivors of childhood ALL should also include neuroimaging when feasible to allow for associations between brain and behavior to be investigated. Longitudinal neuroimaging studies should also be conducted to characterize the progressive change more accurately in brain anatomy and function that occurs in survivors.

Advanced magnetic resonance techniques, such as multishell diffusion imaging and multicompartment diffusion models including neurite orientation dispersion and density imaging, can also be implemented in future studies to examine microscopic white matter network connectivity (69). Additionally, the use of myelin water imaging can build on current knowledge of white matter integrity deficits in survivors by more precisely measuring myelin content. Furthermore, advancements in MRS- or CEST-based imaging may permit future investigators to measure hippocampal neurogenesis, which may play a key role in the neuroanatomical and neurocognitive deficits observed in survivors. Unfortunately, many of the advanced neuroimaging techniques that examine brain connectivity and myelin integrity require scan sequences that are not routinely collected as part of ALL treatment protocols and are often limited to independent research studies. Broad population-based screening using these advanced MRI techniques would greatly benefit pediatric cancer survivors and other clinical populations with high risk for neurological complications, but given their limited accessibility, additional neuroimaging investigations are needed to determine the most viable method for implementing advanced MRI on a larger, clinically relevant scale. The use of multimodality imaging (eg, simultaneous fMRI + EEG) can also be incorporated into future investigations to overcome the limitations of the independent techniques. Combining magnetic resonance-based imaging with other brain imaging modalities such as EEG and fNIRS will be particularly useful for reducing the spatial and temporal constraints typically observed when using a single modality. Considering that EEG and fNIRS systems can be portable and are relatively inexpensive in comparison to other neuroimaging modalities, these techniques may be a particularly useful and cost-effective option for broad-population neurological screening in survivors. A combination of these various brain imaging modalities provides a needed holistic approach to understanding how chemotherapy impacts brain structure and function in long-term survivors of ALL.

Funding

This work was supported by the National Cancer Institute at the National Institutes of Health T32 Institutional Research Training Grant (T32 CA225590 to KRK) and by the American Lebanese Syrian Associated Charities (ALSAC).

Notes

Role of the funders: The funding sources did not have a role in the study design, implementation, or interpretation of the data reported in this systematic review; the preparation or writing of the manuscript; or the decision to submit the findings for publication.

Disclosures: The authors report no conflict of interest.

Author contributions: Conception and design: Kellen Gandy, Kevin R. Krull. Acquisition of data: Kellen Gandy, Molly Littens. Analysis and interpretation of data: All authors. Drafting the manuscript and revising critical content: All authors. Final approval of the manuscript: All authors. Accountable for all aspects of this work: All authors.

Acknowledgements: We thank the researcher investigators who published their studies in the public domain.

Data Availability

The data supporting this manuscript can be provided upon request to the corresponding author.

References

1. Pui C-H, Yang JJ, Hunger SP, et al. Childhood acute lymphoblastic leukemia: progress through collaboration. *J Clin Oncol*. 2015;33(27):2938–2948.
2. Jankovic M, Masera G, Brouwers P, et al. Association of 1800 cGy cranial irradiation with intellectual function in children with acute lymphoblastic leukaemia. *Lancet*. 1994;344(8917):224–227.
3. Gilsanz V, Carlson ME, Roe TF, Ortega JA. Osteoporosis after cranial irradiation for acute lymphoblastic leukemia. *J Pediatr*. 1990;117(2, pt 1):238–244.
4. Rappaport R, Brauner R. Growth and endocrine disorders secondary to cranial irradiation. *Pediatr Res*. 1989;25(6):561–567.

5. Pui C-H, Campana D, Pei D, et al. Treating childhood acute lymphoblastic leukemia without cranial irradiation. *N Engl J Med*. 2009;360(26):2730–2741.
6. Krull KR, Cheung YT, Liu W, et al. Chemotherapy pharmacodynamics and neuroimaging and neurocognitive outcomes in long-term survivors of childhood acute lymphoblastic leukemia. *J Clin Oncol*. 2016;34(22):2644–2653.
7. Fellah S, Cheung YT, Scoggins MA, et al. Brain activity associated with attention deficits following chemotherapy for childhood acute lymphoblastic leukemia. *J Natl Cancer Inst*. 2019;111(2):201–209.
8. Kunin-Batson A, Kadan-Lottick N, Neglia JP. The contribution of neurocognitive functioning to quality of life after childhood acute lymphoblastic leukemia. *Psychooncology*. 2014;23(6):692–699.
9. Myers JS, Pierce J, Pazdernik T. Neurotoxicology of chemotherapy in relation to cytokine release, the blood-brain barrier, and cognitive impairment. *Oncol Nurs Forum*. 2008;35(6):916–920.
10. Kaufmann SH, Earnshaw WC. Induction of apoptosis by cancer chemotherapy. *Exp Cell Res*. 2000;256(1):42–49.
11. Christie L-A, Acharya MM, Parihar VK, Nguyen A, Martirosian V, Limoli CL. Impaired cognitive function and hippocampal neurogenesis following cancer chemotherapy. *Clin Cancer Res*. 2012;18(7):1954–1965.
12. Moher D, Liberati A, Tetzlaff J, Altman DG; for the PRISMA Group. Preferred reporting items for systematic reviews and meta-analyses: the PRISMA statement. *Ann Intern Med*. 2009;151(4):264–269.
13. Whiting P, Savović J, Higgins JP, et al.; for the ROBIS group. ROBIS: a new tool to assess risk of bias in systematic reviews was developed. *J Clin Epidemiol*. 2016;69:225–234.
14. Maillard P, Delcroix N, Crivello F, et al. An automated procedure for the assessment of white matter hyperintensities by multispectral (T1, T2, PD) MRI and an evaluation of its between-centre reproducibility based on two large community databases. *Neuroradiology*. 2008;50(1):31–42.
15. Ashburner J, Friston KJ. Voxel-based morphometry—the methods. *Neuroimage*. 2000;11(6, pt 1):805–821.
16. Mechelli A, Price CJ, Friston KJ, Ashburner J. Voxel-based morphometry of the human brain: methods and applications. *Curr Med Imaging Rev*. 2005;1(2):105–113.
17. Fischl B, Dale AM. Measuring the thickness of the human cerebral cortex from magnetic resonance images. *Proc Natl Acad Sci USA*. 2000;97(20):11050–11055.
18. Ségonne F, Dale AM, Busa E, et al. A hybrid approach to the skull stripping problem in MRI. *Neuroimage*. 2004;22(3):1060–1075.
19. Fischl B, Salat DH, Busa E, et al. Whole brain segmentation: automated labeling of neuroanatomical structures in the human brain. *Neuron*. 2002;33(3):341–355.
20. Fischl B, Salat DH, Van Der Kouwe AJ, et al. Sequence-independent segmentation of magnetic resonance images. *Neuroimage*. 2004;23(suppl 1):S69–S84.
21. Ségonne F, Pacheco J, Fischl B. Geometrically accurate topology-correction of cortical surfaces using nonseparating loops. *IEEE Trans Med Imaging*. 2007;26(4):518–529.
22. Desikan RS, Ségonne F, Fischl B, et al. An automated labeling system for subdividing the human cerebral cortex on MRI scans into gyral based regions of interest. *Neuroimage*. 2006;31(3):968–980.
23. Fischl B, Van Der Kouwe A, Destrieux C, et al. Automatically parcellating the human cerebral cortex. *Cereb Cortex*. 2004;14(1):11–22.
24. Bokde AL, Teipel SJ, Schwarz R, et al. Reliable manual segmentation of the frontal, parietal, temporal, and occipital lobes on magnetic resonance images of healthy subjects. *Brain Res Brain Res Protoc*. 2005;14(3):135–145.
25. Le Bihan D, Mangin JF, Poupon C, et al. Diffusion tensor imaging: concepts and applications. *J Magn Reson Imaging*. 2001;13(4):534–546.
26. Alexander AL, Lee JE, Lazar M, Field AS. Diffusion tensor imaging of the brain. *Neurotherapeutics*. 2007;4(3):316–329.
27. Sarwar T, Ramamohanarao K, Zalesky A. Mapping connectomes with diffusion MRI: deterministic or probabilistic tractography? *Magn Reson Med*. 2019;81(2):1368–1384.
28. Badr MA, Hassan TH, El Gerby KM, Lamey ME-S. Magnetic resonance imaging of the brain in survivors of childhood acute lymphoblastic leukemia. *Oncol Lett*. 2013;5(2):621–626.
29. Banerjee P, Rossi MG, Anghelescu DL, et al. Association between anesthesia exposure and neurocognitive and neuroimaging outcomes in long-term survivors of childhood acute lymphoblastic leukemia. *JAMA Oncol*. 2019;5(10):1456–1463.
30. Billiet T, Elens I, Sleurs C, et al. Brain connectivity and cognitive flexibility in nonirradiated adult survivors of childhood leukemia. *J Natl Cancer Inst*. 2018;110(8):905–913.
31. Cheung YT, Khan RB, Liu W, et al. Association of cerebrospinal fluid biomarkers of central nervous system injury with neurocognitive and brain imaging outcomes in children receiving chemotherapy for acute lymphoblastic leukemia. *JAMA Oncol*. 2018;4(7):e180089.
32. Cheung YT, Sabin ND, Reddick WE, et al. Leukoencephalopathy and long-term neurobehavioural, neurocognitive, and brain imaging outcomes in survivors of childhood acute lymphoblastic leukaemia treated with chemotherapy: a longitudinal analysis. *Lancet Haematol*. 2016;3(10):e456–e466.
33. Duffner PK, Armstrong FD, Chen L, et al. Neurocognitive and neuroradiologic central nervous system late effects in children treated on Pediatric Oncology Group (POG) P9605 (standard risk) and P9201 (lesser risk) acute lymphoblastic leukemia protocols (ACCL0131): a methotrexate consequence? A report from the Children's Oncology Group. *J Pediatr Hematol/Oncol*. 2014;36(1):8–15.
34. Edelmann MN, Krull KR, Liu W, et al. Diffusion tensor imaging and neurocognition in survivors of childhood acute lymphoblastic leukaemia. *Brain*. 2014;137(11):2973–2983.
35. Edelmann MN, Ogg RJ, Scoggins MA, et al. Dexamethasone exposure and memory function in adult survivors of childhood acute lymphoblastic leukemia: a report from the SJLIFE cohort. *Pediatr Blood Cancer*. 2013;60(11):1778–1784.
36. ElAlfy M, Ragab I, Azab I, Amin S, Abdel-Maguid M. Neurocognitive outcome and white matter anisotropy in childhood acute lymphoblastic leukemia survivors treated with different protocols. *Pediatr Hematol Oncol*. 2014;31(2):194–204.
37. Genschaft M, Huebner T, Plessow F, et al. Impact of chemotherapy for childhood leukemia on brain morphology and function. *PLoS One*. 2013;8(11):e78599.
38. Kalafatçılar Aİ, Tüfekçi Ö, Ören H, et al. Assessment of neuropsychological late effects in survivors of childhood leukemia. *Pediatr Hematol Oncol*. 2014;31(2):181–193.
39. Kesler SR, Gugel M, Huston-Warren E, Watson C. Atypical structural connectome organization and cognitive impairment in young survivors of acute lymphoblastic leukemia. *Brain Connect*. 2016;6(4):273–282.
40. Kesler SR, Ogg R, Reddick WE, et al. Brain network connectivity and executive function in long-term survivors of childhood acute lymphoblastic leukemia. *Brain Connect*. 2018;8(6):333–342.
41. Kesler SR, Tanaka H, Koovakkattu D. Cognitive reserve and brain volumes in pediatric acute lymphoblastic leukemia. *Brain Imaging Behav*. 2010;4(3-4):256–269.
42. Phillips NS, Cheung YT, Glass JO, et al. Neuroanatomical abnormalities related to dexamethasone exposure in survivors of childhood acute lymphoblastic leukemia. *Pediatr Blood Cancer*. 2020;67(3):e27968.
43. Reddick WE, Shan ZY, Glass JO, et al. Smaller white-matter volumes are associated with larger deficits in attention and learning among long-term survivors of acute lymphoblastic leukemia. *Cancer*. 2006;106(4):941–949.
44. Reddick WE, Taghipour DJ, Glass JO, et al. Prognostic factors that increase the risk for reduced white matter volumes and deficits in attention and learning for survivors of childhood cancers. *Pediatr Blood Cancer*. 2014;61(6):1074–1079.
45. Sabin ND, Cheung YT, Reddick WE, et al. The impact of persistent leukoencephalopathy on brain white matter microstructure in long-term survivors of acute lymphoblastic leukemia treated with chemotherapy only. *Am J Neuroradiol*. 2018;39(10):1919–1925.
46. van der Plas E, Schachar RJ, Hitzler J, et al. Brain structure, working memory and response inhibition in childhood leukemia survivors. *Brain Behav*. 2017;7(2):e00621.
47. Zając-Spychała O, Pawlak MA, Karmelita-Katulska K, Pilarczyk J, Derwich K, Wachowiak J. Long-term brain structural magnetic resonance imaging and cognitive functioning in children treated for acute lymphoblastic leukemia with high-dose methotrexate chemotherapy alone or combined with CNS radiotherapy at reduced total dose to 12 Gy. *Neuroradiology*. 2017;59(2):147–156.
48. Zając-Spychała O, Pawlak M, Karmelita-Katulska K, et al. Anti-leukemic treatment-induced neurotoxicity in long-term survivors of childhood acute lymphoblastic leukemia: impact of reduced central nervous system radiotherapy and intermediate-to high-dose methotrexate. *Leuk Lymphoma*. 2018;59(10):2342–2351.
49. Jamroziak K, Robak T. Pharmacogenomics of MDR1/ABCB1 gene: the influence on risk and clinical outcome of haematological malignancies. *Hematology*. 2004;9(2):91–105.
50. Dietrich J, Han R, Yang Y, Mayer-Pröschel M, Noble M. CNS progenitor cells and oligodendrocytes are targets of chemotherapeutic agents in vitro and in vivo. *J Biol*. 2006;5(7):22–23.
51. Conklin KA. Chemotherapy-associated oxidative stress: impact on chemotherapeutic effectiveness. *Integr Cancer Ther*. 2004;3(4):294–300.
52. Engelhardt M, Ozkaynak M, Drullinsky P, et al. Telomerase activity and telomere length in pediatric patients with malignancies undergoing chemotherapy. *Leukemia*. 1998;12(1):13–24.
53. Lee J-J, Nam C-E, Cho S-H, Park K-S, Chung I-J, Kim H-J. Telomere length shortening in non-Hodgkin's lymphoma patients undergoing chemotherapy. *Ann Hematol*. 2003;82(8):492–495.
54. Maccormick RE. Possible acceleration of aging by adjuvant chemotherapy: a cause of early onset frailty? *Med Hypotheses*. 2006;67(2):212–215.
55. Shi D-D, Huang Y-H, Lai CSW, et al. Chemotherapy-induced cognitive impairment is associated with cytokine dysregulation and disruptions in neuroplasticity. *Mol Neurobiol*. 2019;56(3):2234–2243.
56. Michaud M, Balardy L, Moulis G, et al. Proinflammatory cytokines, aging, and age-related diseases. *J Am Med Dir Assoc*. 2013;14(12):877–882.
57. Sawada H, Ibi M, Kihara T, Urushitani M, Akaike A, Shimohama S. Estradiol protects mesencephalic dopaminergic neurons from oxidative stress-induced neuronal death. *J Neurosci Res*. 1998;54(5):707–719.
58. Chisu V, Manca P, Lepore G, Gadau S, Zedda M, Farina V. Testosterone induces neuroprotection from oxidative stress. Effects on catalase activity and 3-nitro-L-tyrosine incorporation into alpha-tubulin in a mouse neuroblastoma cell line. *Archives Italiennes de Biologie*. 2006;144(2):63–73.
59. Lee D-C, Im J-A, Kim J-H, Lee H-R, Shim J-Y. Effect of long-term hormone therapy on telomere length in postmenopausal women. *Yonsei Med J*. 2005;46(4):471–479.

60. Monje ML, Vogel H, Masek M, Ligon KL, Fisher PG, Palmer TD. Impaired human hippocampal neurogenesis after treatment for central nervous system malignancies. *Ann Neurol*. 2007;62(5):515–520.
61. Giedd JN, Blumenthal J, Jeffries NO, et al. Brain development during childhood and adolescence: a longitudinal MRI study. *Nat Neurosci*. 1999;2(10):861–863.
62. Vijayakumar N, Allen NB, Youssef G, et al. Brain development during adolescence: a mixed-longitudinal investigation of cortical thickness, surface area, and volume. *Hum Brain Mapp*. 2016;37(6):2027–2038.
63. De Bellis MD, Keshavan MS, Beers SR, et al. Sex differences in brain maturation during childhood and adolescence. *Cereb Cortex*. 2001;11(6):552–557.
64. Tamnes CK, Østby Y, Fjell AM, Westlye LT, Due-Tønnessen P, Walhovd KB. Brain maturation in adolescence and young adulthood: regional age-related changes in cortical thickness and white matter volume and microstructure. *Cereb Cortex*. 2010;20(3):534–548.
65. Lebel C, Walker L, Leemans A, Phillips L, Beaulieu C. Microstructural maturation of the human brain from childhood to adulthood. *Neuroimage*. 2008;40(3):1044–1055.
66. Moore-Maxwell CA, Datto MB, Hulette CM. Chemotherapy-induced toxic leukoencephalopathy causes a wide range of symptoms: a series of four autopsies. *Mod Pathol*. 2004;17(2):241–247.
67. Baehring J, Fulbright R. Delayed leukoencephalopathy with stroke-like presentation in chemotherapy recipients. *J Neurol Neurosurg Psychiatry*. 2008;79(5):535–539.
68. Sapolsky RM. Glucocorticoids and hippocampal atrophy in neuropsychiatric disorders. *Arch Gen Psychiatry*. 2000;57(10):925–935.
69. Zhang H, Schneider T, Wheeler-Kingshott CA, Alexander DC. NODDI: practical in vivo neurite orientation dispersion and density imaging of the human brain. *Neuroimage*. 2012;61(4):1000–1016.